

# Chapter 3

## Evolution of Microstructure in Semisolid Alloys During Isothermal Holding (Soaking)

### 3.1 Introduction

In a recent review of coarsening, Flemings [19] states that this process refers to the growth “of solid regions of low curvature at the expense of regions of higher curvature,” and this includes “the growth of larger particles or dendrite arms with the simultaneous dissolution of smaller particles or arms (so-called ‘ripening’), the filling of spaces between particles or dendrite arms (‘coalescence’) and the break-up of dendrites (‘dendrite multiplication’).” This is a view adopted in the present chapter. The driving force is of course always the reduction of total solid–liquid interface area and the reduction in the associated interfacial energy, and the general mechanism by which this is achieved is diffusion of solute atoms through the liquid from concentration gradients established between regions of high and low curvature. Owing to the complex geometries that may exist in coarsening semisolid systems with competing fluxes between different particles, which can change with both time and place, simple kinetic equations to describe the overall coarsening process is probably not possible. However, where the geometry of the solid may be clearly described, for instance in terms of dendrite arms formed early in solidification, simple kinetics can be derived. More complex geometries may develop later during coarsening that are more difficult to provide with an adequate geometrical description.

It is convenient (and to some extent accurate) to distinguish further between two coarsening processes occurring during the isothermal soaking of dendritic or near dendritic microstructures: spheroidization and ripening. The former precedes ripening, and involves the melting back or thinning of dendrite arms, and in some cases, their melting off [7], as a result of high surface curvatures and short diffusion distances providing high solute gradients in the liquid around the grain. The negative surface curvature at the dendrite root is in contact with high solute in the liquid, whereas at the tip the liquid is poor in solute, giving rise to these gradients. Consider a fine dendritic particle of  $100\ \mu\text{m}$  size, coarsening isothermally by the arms melting back from their tips to form eventually a spheroid or globule of approximately similar diameter. When the arm spacing  $\lambda$  is of the same order as the particle size, the dendritic structure has effectively disappeared and replaced by a globular

particle. This will occur for  $\lambda = 100 \mu\text{m}$  in a time  $t_0 = mHC(1-k)\lambda^3/128D\sigma T$  [20], where  $C$  is the solute concentration in the liquid,  $k$  the partition coefficient,  $H$  the heat of fusion,  $T$  the absolute temperature,  $\sigma$  the surface energy, and  $m$  the liquidus slope. Using data from the Al–4.5%Cu system [20],  $t_0$  is determined to be about 6 min. Although this is a rough calculation, it does indicate that in the period of ingot soaking in the semisolid state, there is time for fine dendrite structure on the scale above to develop spheroidal shapes. This stage of coarsening only involves *intragranular* diffusion (i.e., in the liquid within the dendrite) and the grain density remains essentially constant.

Once the dendrite structure has effectively disappeared (but before spheroidization is fully completed), the second process of Ostwald ripening can begin, which involves the diffusion of solute in the liquid *between* grains (*intergranular* diffusion). This is a slower process because interface curvatures are less than in dendritic structures, and diffusion distances are greater, both leading to lower solute fluxes. The classical analysis of this situation for widely separated spherical particles in a stagnant matrix is due to Lifshitz and Slyzov [21] and Wagner [22] (LSW theory), and predicts cubic behavior with time:  $d^3 - d_0^3 = k_2t$ , where  $d$  is the particle diameter at time  $t$ , and  $d_0$  is the initial diameter. Using the value of  $k_2$  determined by Loué and Suéry [13], and  $d_0 = 100 \mu\text{m}$ , the particle diameter after 1 h is  $115 \mu\text{m}$ , which may be regarded as negligible growth for thixoforming purposes. However, this neglects coarsening by coalescence of particles by collision and joining together, which may be important in some situations (see Sect. 3.4).

## 3.2 Coarsening in Al–Cu Alloys

Most of the early experimental work in this field of coarsening was carried out on Al/Cu alloys much by Flemings et al. [23] following their original work on solidification structures. Kattamis et al. [24, 25] have more recently added to this literature, again investigating the changes in morphology of directionally solidified dendritic structures during solidification, as well as examining changes during isothermal treatment of sections. It was observed that under isothermal conditions, the dendrite structure fragmented after about 30 min, thereafter forming a spheroidal particle structure which subsequently coarsened very slowly. Using standard optical metallography techniques, they obtained information on changes of secondary arm spacings ( $\lambda$ ) and the total surface area per unit volume ( $S_v$ ) as a function of time. Both parameters agreed satisfactorily with different geometrical models [20, 25] based on diffusion of the solute in the liquid from regions of high curvature to those of low, and demonstrated that copper diffusion was the rate-controlling step.

The work of Poirier et al. [26] using grain refined Al–15.6 wt% Cu alloy, had a fine equiaxed dendritic structure initially, whose secondary arm spacing rapidly increased with isothermal holding time until the grains developed an essentially globular shape after around 20 min, depending on the original fineness. The arm

spacing increase followed a  $t^{1/3}$  time law, again consistent with solute diffusion from the dendrite tips resulting in their melting (dissolving) back. Subsequent coarsening of the globular particles was again slow with  $S_v \propto t^{-1/n}$ , where  $n > 5$ . This is clearly much slower than predicted by the LSW theory of ripening, which assumes growth of separated particles by diffusion through the matrix and it was felt to imply coalescence in which particles join together.

### 3.3 Coarsening in Al–Si Alloys

The much of the work carried out to investigate the change in microstructure during isothermal holding has been directed to the Al–7Si alloys, A356, and 357. These are the alloys most commonly used in commercial thixoforming that produce around  $f_s \sim 0.5$  on melting the Al–Si eutectic at 577°C. It is clearly of great practical importance to understand the conditions in which ideal thixoforming structures may be formed, that is possessing fine spheroidal or globular solid particles within a liquid matrix.

A key investigation in this area is that of Loué and Suery [13], in which  $S_v$ ,  $N_a$ , and the shape factor  $F_g$  were measured as a function of time at 580°C ( $f_s = 0.45$ ) in alloy produced by DC casting, with and without electromagnetic stirring (MHD). The difference in initial microstructure and after isothermal holding for 5 min and 15 h is shown in Fig. 3.1, revealing a highly dendritic structure in the conventional unstirred casting compared to the degenerate structure in the MHD casting. The measurements of  $S_v$  and  $N_a$  are shown in Fig. 3.2a, b, respectively, for times up to 1500 min (about 1 day), the former indicating surprisingly little difference between the two production routes. However, the grain density,  $N_a$ , falls dramatically in the MHD material, but remains effectively constant in the conventional casting. A further difference in behavior can be observed in the shape factor  $F_g$  (see Fig. 3.2c), where it is very clear that the MHD structure rapidly spheroidizes within 30 min, whereas the conventional casting still has a complex morphology even after 24 h. These results have been interpreted as indicating that the first process to occur during isothermal holding of semisolid structures is the disappearance of dendrite arms within each grain, either by melting back of short arms, or by the coalescence of neighboring arms of the same grain that necessarily have the same crystallographic orientation and may lead to the entrapment of liquid between longer dendrite arms. Clear evidence of both these processes were obtained in the early work of Chien and Kattamis [27] and particularly from the quenched steady state growth of Al–Cu alloys of Young and Kirkwood [28]. Both are diffusional processes driven by solute differences in the liquid originating from the curvature of the interface and lead eventually to spheroidization accompanied by removal of entrapped liquid and an overall reduction of surface area in the system. Only after a degree of spheroidization with the removal of entrapped liquid has been achieved, however, the process of grain coarsening can begin, in which the smaller grains

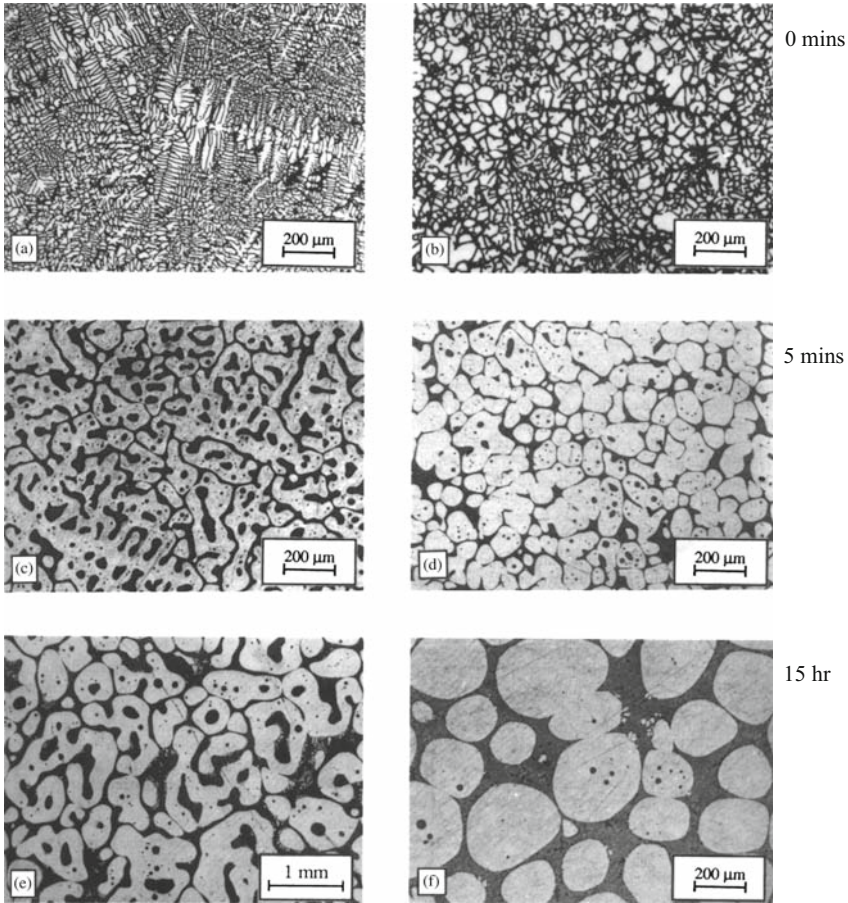


**Fig. 3.1** (a, c, e) Conventional casting after 0 min, 5 min, and 15 h soaking, (b, d, f) MHD casting after 0 min, 5 min, and 15 h soaking

disappear as the larger ones grow by solute diffusion (Ostwald ripening) or by the coalescence of freely moving individual grains or agglomerates to form even larger agglomerates, leading to a fall in  $N_a$ . This is why the highly dendritic morphology of the conventionally cast structure maintains a constant grain density shown in Fig. 3.2b.

Tzimas and Zavaliangos [29] have also examined the microstructural changes in this alloy, as prepared by electromagnetic stirring, occurring during the first 5 min of isothermal treatment at  $f_s = 0.45$ , which covers the period of time normally used in industrial practice. They observed different initial microstructures within the cast billet, which had a highly dendritic columnar structure at the perimeter, whereas the center consisted of “rosette”-shaped particles. It is postulated that these rosettes

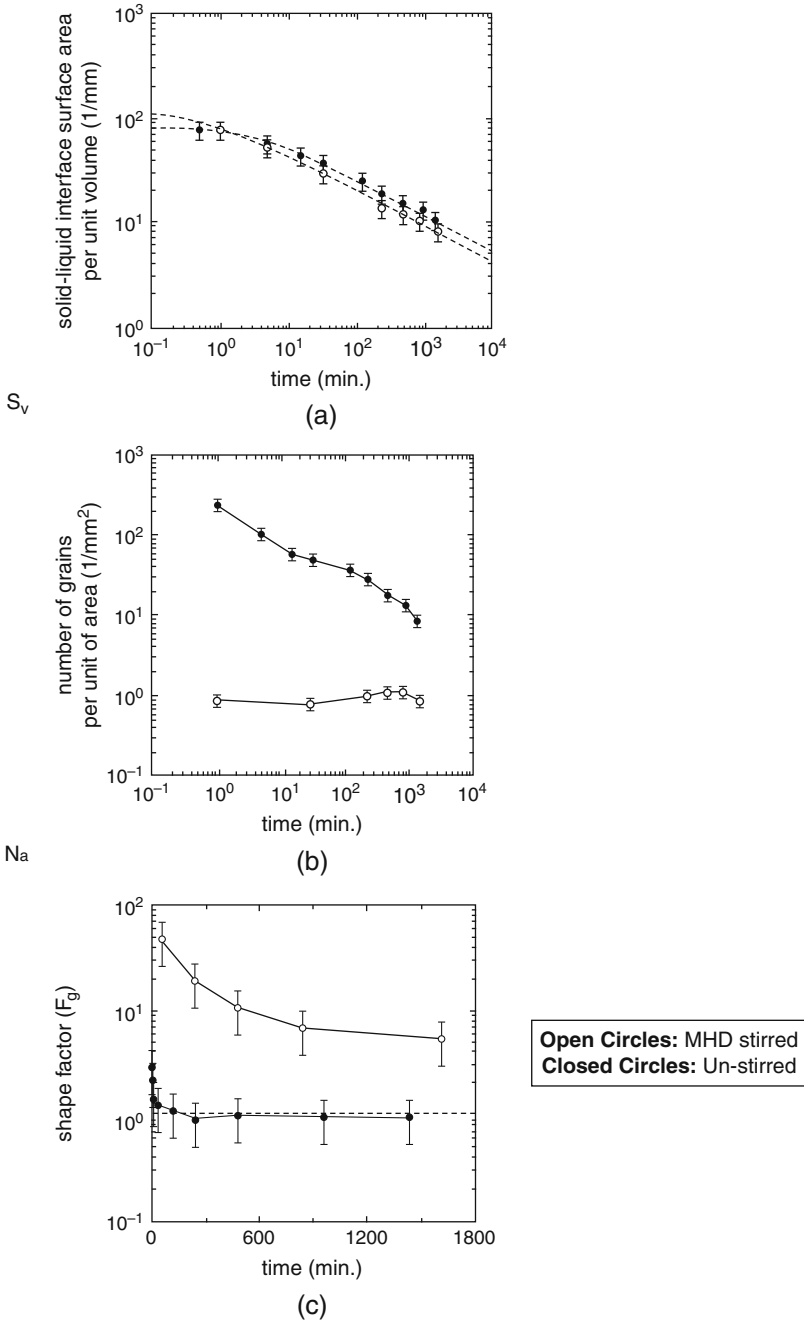
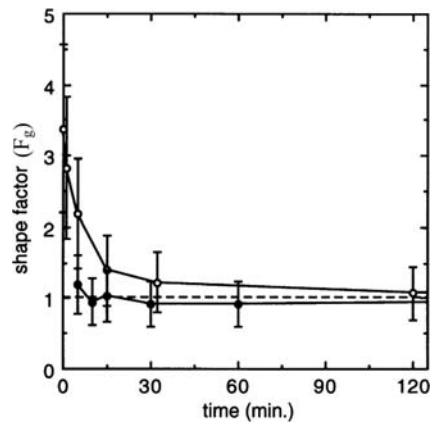


Fig. 3.2 Microstructural changes in DC cast Al/7%Si Alloys during isothermal heat treatment at 580 degC.

are created in the solidification process as a result of the circulation of the fluid within the ingot sump generated by the moving electromagnetic field that detaches dendrite arms from the growing perimeter region and circulates them into the hot sump center. Here, they partially melt and spheroidize initially to form rosettes, and in the process of circulating within the central sump, they collide and join together where the grain orientations are favorable to form agglomerates of rosettes having low energy boundaries separating the grains. These agglomerates or clusters are eventually deposited at the inward growing solid wall of the billet. The clusters of rosette-shaped grains can contribute to the rapid coarsening of grains during isothermal treatment in the semisolid state through the elimination of low angle boundaries by migration or rotation of the grains within the cluster. The shape factor ( $F_0$ ) in both structural regions shows a rapid decrease in the first few minutes (as with Loué and Suery) so that little difference exists between perimeter and interior, in both shape and grain size. Allowing for the different measures of shape factor, the agreement on grain size and morphology between the two investigations is quite satisfactory: within the first few minutes of isothermal treatment, rapid spheroidization of the grains takes place with limited grain growth (from 70 to 100  $\mu\text{m}$ ). This is quite acceptable for thixoforming. In contrast to this, the shape factor in conventional unstirred DC billets in these short times (and even in much longer periods) is very high, and would not be suitable.

Other production routes to form appropriate semisolid slurries in this alloy system have been investigated by both these researchers. By cold working, followed by recrystallization and partial melting (SIMA route [30]), Loué and Suery [13] showed that cold work resulting from 25% reduction in section led to a reduction in grain size down to 55  $\mu\text{m}$ , irrespective of the starting grain size; further cold work had no apparent effect. The evolution of the shape factor  $F_g$  of the SIMA material as compared to MHD alloy is shown in Fig. 3.3, and reveals that spheroidization is even more rapid, essentially being achieved in less than 5 min isothermal holding. This is attributed to the initial small grain size and nondendritic morphology of the partially melted microstructure. Furthermore, it was shown that the coarsening rate at 580°C



**Fig. 3.3** Effect of Cold Work on particle spheroidisation (closed circles) compared to undeformed alloy (open circles).

of the SIMA alloy was lower than that of the MHD for these essentially spheroidal particles, and greater than expected from Ostwald ripening alone. It was therefore suggested that the coalescence of particles or aggregates must play a significant part in growth, and that the clustering of particles with low energy grain boundaries (see earlier section) as expected in MHD, might explain the higher coarsening rate seen in this material.

Similar findings to the above were reported by Tzimas and Zavaliangos [29] in alloy, which had been heavily warm worked before partial melting (RAP route), although this resulted in a larger grain size ( $90\ \mu\text{m}$ ). However, no grain growth could be observed during isothermal holding in the semisolid state over 5 min, nor was any shape factor change reported.

Finally, the effect of grain refinement and spray casting as fine grained source material for thixoforging was examined by these workers in view of the fact that small grains should spheroidize more rapidly. This was demonstrated using a grain refined alloy with  $\text{Ti}_5\text{B}$  addition to a permanent mould casting. The shape factor was significantly reduced after isothermal holding below that without refinement after 35 min, but still well above that for the MHD stirred material however. The spray cast alloy generates the finest grain size of all,  $40\ \mu\text{m}$  near-spherical particles in this alloy system, although since the diameter increases to  $70\ \mu\text{m}$  in 5 min, it is not clear that this is a great benefit in thixoforging given the inevitable increased cost of the source alloy.

A disadvantage in studying the Al–7Si alloy system is that 50% volume fraction liquid is formed immediately on melting the eutectic, which prevents studies on  $f_s$  of greater than 0.5. Using Al–4Cu alloy, Tzimas and Zavaliangos investigated the short time coarsening of spherical particles from both SIMA and spray-cast sources at  $f_s = 0.6$  and  $f_s = 0.9$ . The results indicated that the spray-cast alloy coarsened more slowly and that, contrary to prediction, the high fraction solid slurry coarsened the slowest. This might be explained in terms of coarsening by particle coalescence involving the rotation of grains to form low energy boundaries and their migration. Where grains are initially random in orientation to one another, as in spray-casting, this is a slow process. Furthermore, where fine insoluble precipitates or gas pores exist within the solid, as noted in some spray-deposited alloy, this will further hinder grain boundary migration and the coarsening process.

### 3.4 X-ray Microtomography of Alloy Slurries

Microstructural changes occurring during the isothermal treatment of semisolid slurries in most investigations have involved quenching followed by sectioning. The problem with this procedure is, firstly, the quenching is never rapid enough to prevent further growth of the solid so affecting microstructural measurements, and, secondly, solids that are connected in 3D, may not be revealed as such in a 2D section. Serial sectioning [31] carried out to investigate this is limited by the fineness of sectioning that can be mechanically performed.

X-ray microtomography overcomes both these limitations by employing a high intensity X-ray beam generated using a synchrotron to penetrate through a small sample and recorded by a high speed digital camera [32]. Using this set-up, the microstructure can be continuously scanned (without quenching) during isothermal treatment, and a scan can be carried out every minute on the same small volume (during which negligible change is observed), in which the change of microstructure with time may be recorded with a spatial resolution of better than  $3 \mu\text{m}$ .

Suery et al. [33] have used this technique at Grenoble to investigate microstructural changes during the partial melting of Al-15.8% Cu alloy, held at  $555^\circ\text{C}$  in the semisolid region for up to 80 min. Over this period, a number of global measurements were made on a specific volume within the sample: the number of particles per unit volume ( $N_v$ ), the mean shape factor, the average coordination factor, the average particle volume ( $V$ ) and effective radius ( $R$ ), and the particle surface area per unit volume ( $S_v$ ).

One surprising result was the coordination number of each particle (the continuity factor  $\bar{m}$  in Sect. 2.3) with neighboring particles in an undisturbed sample, which revealed that there are no free unattached particles but most on average are connected to six or seven neighbors. This probably explains the initial apparent yield point in undisturbed slurries. Other significant results were:

1. The volume fraction solid with time, showing an increase in the first 30 min after which it levels out. This is attributed to diffusion in the solid leading eventually to complete equilibrium between solid and liquid, and the absorption of entrapped liquid within the particles. It was also shown that in quenched samples there was 20% greater solid than the nonquenched, revealing the possible large error introduced by quenching
2. The shape factor, determined from  $6V\sqrt{(\pi/S^3)}$  where  $V$  is the volume and  $S$  the surface area of the particle, and is 1 for a sphere. The mean value rises rapidly from 0.66 to 0.82 in 25 min, and then slowly to 0.85, but complete spheroidization is not achieved

Since it is clear that the averaged values of  $N_v$  or  $S_v$  cannot establish the coarsening process unambiguously, attention was directed by these authors to measure the changes occurring locally between particular particles, and the growth or shrinkage of the necks between them. Two general extreme types of behavior were observed: (1) that between particles of very different sizes in which the smaller shrinks continuously with time in a process similar to Ostwald ripening, feeding larger neighbors (Fig. 3.4); and (2) that between particles of essentially equal size resulting in their coalescence eventually into a single particle (Fig. 3.5). In the latter case, the contact area of the neck grows continuously with time, whereas in the former it decreases. However, there are many intermediate situations in which the neck first grows then shrinks, or even remains static. These diverse behaviors are no doubt the consequence of the complex and changing particle environments, and make the description of coarsening in terms of simple global kinetic equations impossible. However, it would appear that the morphological changes are all driven by solute diffusion through the liquid matrix by gradients established by local surface



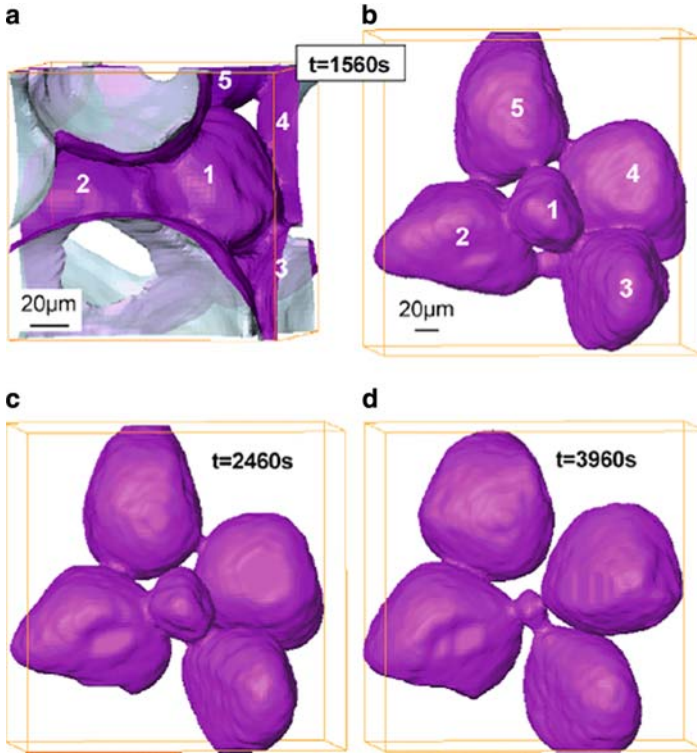


**Fig. 3.4** Observations of neck representative of trend with unequal sized particles

curvature. Furthermore, the finer morphologies, such as dendrite arms and small particles will coarsen rapidly and disappear first because of their associated higher curvatures.

The plots of  $1/N_v$  and  $V$  against time both indicate a change in kinetics in this work at around 50 min: The average particle volume  $V$  increased linearly with time up to this point (see Fig. 3.6) before falling off. The linear portion indicates a  $t^{1/3}$  growth in radius that is consistent with ripening involving the absorption of small particles by larger neighbors by a process akin to Ostwald ripening as proposed by Courtney [34]. The particle density ( $N_v$ ) changes as  $1/t$  up to 50 min, which is also consistent with a ripening process, thereafter the rate of particle removal decreases presumably because the smaller particles have disappeared by absorption, and the dominant process is now the coalescence of essentially equally sized particles – a much slower process, because of lower solute diffusion gradients. This would account for the slower growth of the average particle volume  $V$  and radius  $R$  in Fig. 3.6 after 50 min. Also, a slower growth rate is obtained in fitting  $S_v$  as a function of time where the time exponent is around  $1/7$ . The explanation for this low exponent is not entirely clear but it is suggested that the influence of neighboring particles, with complex and competing diffusion fields must be involved at this later stage in

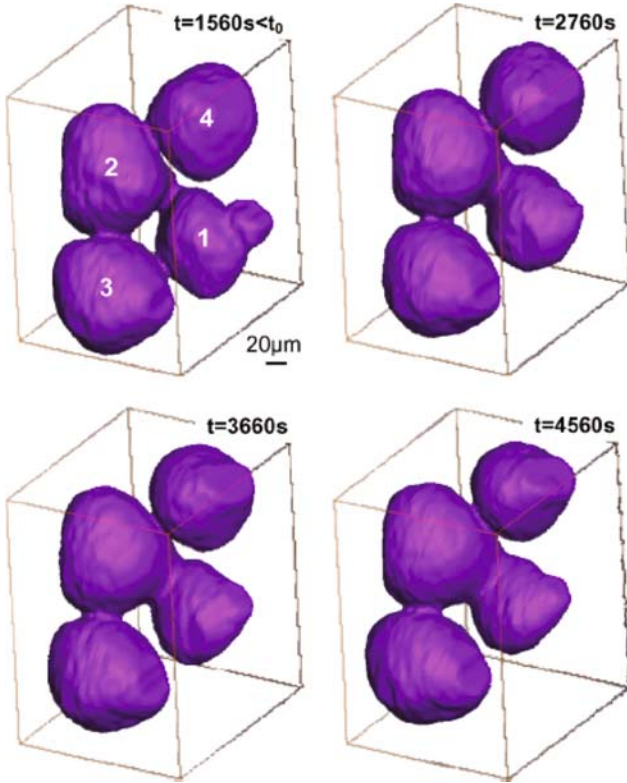


Fig. 3.5 Observations of neck representative of trend for equal sized particles

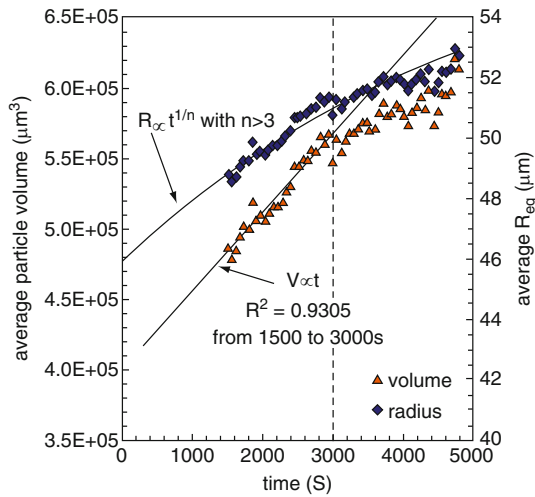


Fig. 3.6 Variation of the average solid particle volume and equivalent radius with isothermal holding time

coarsening. The rate of growth of the necks between particles was also examined by X-ray microtomography. It was found that the average neck radius increased with time as  $t^{1/5.8}$ . Also, a number of individual necks were measured and the average of the continuously growing necks (i.e., those exhibiting pure coalescence) increased as  $t^{1/4.8}$ . Both are close to the value, predicted by Courtney of  $t^{1/5}$ , based on diffusion of solute through the matrix to the neck formed between two particles of equal size.

A more detailed account of the results and interpretation of this work are given in [33].